JPET Fast Forward. Published on April 19, 2011 as DOI:10.1124/jpet.111.180257

JPET #180257

Mechanistic and pharmacological characterization of PF-04457845: a highly potent and selective FAAH inhibitor that reduces inflammatory and noninflammatory pain

Kay Ahn, Sarah E. Smith, Marya B. Liimatta, David Beidler, Nalini Sadagopan, David T. Dudley, Tim Young, Paul Wren, Yanhua Zhang, Steven Swaney, Keri Van Becelaere, Jacqueline L. Blankman, Daniel K. Nomura, Shobha N. Bhattachar, Cory Stiff, Tyzoon K. Nomanbhoy, Eranthie Weerapana, Douglas S. Johnson, and Benjamin F. Cravatt.

Pfizer Worldwide Research and Development, Groton, CT 06340, USA (K.A., Y.Z., C.S., D.S.J.); Ann Arbor, MI 48105, USA (K.A., S.E.S., M.B.L., D.B. N.S., D.T.D., Y.Z., S.S., K.V.B., S.N.B., C. S., D.S.J.); Cambridge, Massachusetts 63017, USA (D.B.); Sandwich, Kent, CT13 9NJ, UK (T.Y., P.W.); ActivX Biosciences, 11025 North Torrey Pines Road, La Jolla, CA 92037, USA (T.K.N.); and The Skaggs Institute for Chemical Biology and Department of Chemical Physiology, The Scripps Research Institute, 10550 N. Torrey Pines Rd. La Jolla, CA 92037, USA (J.L.B., D.K.N., E.W., B.F.C.)

Copyright 2011 by the American Society for Pharmacology and Experimental Therapeutics.

1. Running title: PF-04457845, a highly potent and selective FAAH inhibitor

2. Corresponding Author

Kay Ahn, Ph.D.

Pfizer Worldwide Research and Development

Mail Box: 8220-3373

Eastern Point Road

Groton, CT 06340

USA

Tel: 860-686-9406

Fax: 860-441-0548

E-mail: kay.ahn@pfizer.com

3. Number of text pages: 41

   Number of tables: 2

   Number of figures: 10

   Number of references: 40

   Number of words in Abstract: 250

   Number of words in Introduction: 711

Number of words in Discussion: 689

4. Abbreviations: ABPP, activity-based protein profiling; AEA, Anandamide; CB1, CB1 cannabinoid receptor; CB2, CB2 cannabinoid receptor; CC, click chemsitry; CFA, complete Freund's adjuvant; endocannabinoid, endogenous cannabinoid; FAAH, fatty acid amide hydrolase; FP, fluorophosphonate; FP-rhodamine, fluorophosphonate carboxytetramethylrhodamine; MIA, Monosodium iodoacetate; NAE, *N*-acyl ethanolamine; NADH, nicotinamide adenine dinucleotide (reduced form); NAD+, nicotinamide adenine dinucleotide (oxidized form); OEA, *N*-oleoyl ethanolamine; PEA, *N*-palmitoyl ethanolamine; PWT, paw withdrawal threshold; THC, Δ^9-tetrahydrocannabinol.

5. Recommended section assignment: Drug Discovery and Translational Medicine

Abstract

The endogenous cannabinoid (endocannabinoid) anandamide is principally degraded by the integral membrane enzyme fatty acid amide hydrolase (FAAH). Pharmacological blockade of FAAH has emerged as a potentially attractive strategy to augment endocannabinoid signaling and retain the beneficial effects of cannabinoid receptor activation, while avoiding the undesirable side effects, such as weight gain and impairments in cognition and motor control, observed with direct cannabinoid receptor 1 agonists. Here, we report the detailed mechanistic and pharmacological characterization of PF-04457845, a highly efficacious and selective FAAH inhibitor. Mechanistic studies confirm that PF-04457845 is a time-dependent, covalent FAAH inhibitor that carbamylates FAAH's catalytic serine nucleophile. PF-04457845 inhibits human FAAH with high potency (k_{inact}/K_i = 40300 $M^{-1}s^{-1}$; IC_{50} = 7.2 nM) and is exquisitely selective in vivo as determined by activity-based protein profiling. Oral administration of PF-04457845 produced potent antinociceptive effects in both inflammatory (complete Freund's adjuvant (CFA)) and noninflammatory (monosodium iodoacetate (MIA)) pain models in rats, with a minimum effective dose of 0.1 mg/kg (CFA model). PF-04457845 displayed a long duration of action as a single oral administration at 1 mg/kg showed in vivo efficacy for 24 hr with a concomitant near complete inhibition of FAAH activity and maximal sustained elevation of anandamide in brain. Significantly, PF-04457845-treated mice at 10 mg/kg elicited no effect in motility, catalepsy, and body temperature. Based on its exceptional selectivity and in vivo efficacy, combined with long duration of action and optimal pharmacokinetic properties, PF-04457845 is a clinical candidate for the treatment of pain and other nervous system disorders.

Introduction

Fatty acid amide hydrolase (FAAH) is an integral membrane enzyme that hydrolyzes the fatty acid amide family of lipid transmitters including the endogenous cannabinoid (endocannabinoid) *N*-arachidonoyl ethanolamine (anandamide, AEA) (Cravatt et al., 1996; McKinney and Cravatt, 2005; Ahn et al., 2008). AEA is one of two principal endocannabinoids identified in mammals that activate the cannabinoid receptors CB1 and CB2, which are also activated by Δ^9-tetrahydrocannabinol (THC), the psychoactive substance in marijuana (Mechoulam, 1986). Although the medically beneficial properties of THC and other CB1 agonists, which include pain relief, have long been recognized, their broad clinical utility has been limited due to undesirable side effects, such as weight gain and impairments in cognition and motor control. In contrast, FAAH(-/-) mice and mice treated with FAAH inhibitors have been found to display analgesia (Cravatt et al., 2001; Kathuria et al., 2003; Lichtman et al., 2004; Chang et al., 2006; Jayamanne et al., 2006; Russo et al., 2007; Ahn et al., 2009; Kinsey et al., 2009; Naidu et al., 2010), anti-inflammation (Cravatt et al., 2004; Massa et al., 2004; Holt et al., 2005), anxiolysis (Kathuria et al., 2003; Naidu et al., 2007; Kinsey et al., 2010), sleep-enhancement (Huitron-Resendiz et al., 2004), and antidepression (Gobbi et al., 2005; Naidu et al., 2007) without the untoward side effects observed with direct CB1 agonists (Cravatt et al., 2001; Kathuria et al., 2003; Lichtman et al., 2004; Ahn et al., 2009). These data suggest that FAAH/AEA pathways regulate a discrete subset of behavioral processes affected by direct CB1 agonists. Therefore, the selective pharmacological inhibition of FAAH has emerged as an exciting potential strategy to increase 'endocannabinoid tone' and retain the beneficial effects of cannabinoid receptor activation, while avoiding the undesirable effects of direct CB1 agonists.

FAAH belongs to the amidase signature class of enzymes, a subclass of serine hydrolases that has an unusual Ser-Ser-Lys catalytic triad (Ser241-Ser217-Lys142 in FAAH) (Patricelli et al., 1999; McKinney and Cravatt, 2003). FAAH hydrolyzes several lipid signaling molecules in addition to AEA, including the anti-inflammatory and analgesic factor *N*-palmitoyl ethanolamine (PEA) (Lambert et al., 2002), the sleep-inducing substance 9(*Z*)-octadecenamide (oleamide) (Cravatt et al., 1995), and the satiating signal *N*-oleoyl ethanolamine (OEA) (Rodriguez de Fonseca et al., 2001). Unlike AEA, these lipid transmitters (PEA, oleamide, and OEA) exert their biological activities *via* non-cannabinoid receptor pathways.

There have been significant advances in the development of FAAH inhibitors over the past several years, including both reversible and irreversible covalent inhibitors. The α-ketoheterocycles such as OL-135 inhibit FAAH through a reversible hemiketal formation with the active site Ser241 (Boger et al., 2005; Mileni et al., 2009). Carbamates such as URB597 inhibit FAAH by an irreversible, covalent mechanism involving carbamylation of Ser241 (Kathuria et al., 2003; Alexander and Cravatt, 2005). We have previously reported a series of piperidine/piperazine urea FAAH inhibitors, exemplified by PF-750 and PF-3845, that inhibit FAAH with high selectivity (Ahn et al., 2007; Mileni et al., 2008; Ahn et al., 2009; Johnson et al., 2009). Mechanistic and X-ray crystallographic studies revealed that these piperidine ureas, despite the inherent stability of the urea functional group, inhibit FAAH in a time-dependent manner involving carbamylation of FAAH's catalytic Ser241 nucleophile (Ahn et al., 2007; Mileni et al., 2008; Ahn et al., 2009). We have recently described the evolution of this piperidine urea series of FAAH inhibitors to create compounds with improved potency and pharmaceutical

properties, culminating in the identification of the clinical candidate PF-04457845 (Johnson et al., 2011).

In this report, we describe a detailed mechanistic and pharmacological characterization of PF-04457845. We show that PF-04457845 is exquisitely selective for FAAH both in vitro and in vivo. Furthermore, we report a detailed evaluation of PF-04457845 in rat models of acute, inflammatory pain and chronic, noninflammatory pain. Importantly, we show a tight relationship between the in vivo efficacy and modulation of FAAH activity and its substrates (*N*-acyl ethanolamines, NAEs) from blood leukocytes/plasma, which have the potential to serve as translatable biomarkers for clinical trials. Furthermore, we report that PF-04457845 elicits no effect in motility, catalepsy, and body temperature. Our data indicate that PF-04457845 displays an unprecedented combination of in vitro potency, in vivo efficacy, selectivity, long duration of action, and pharmaceutical properties, leading to its selection as a clinical candidate for the treatment of pain and other nervous system disorders.

Methods

Materials. PF-04457845 was synthesized as recently described (Johnson et al., 2011). URB597 and JP104 were purchased from Cayman Chemicals (Ann Arbor, MI). Inhibitors were stored as dry powders at RT and dissolved in DMSO to prepare concentrated stock solutions for the *in vitro* potency measurements. SR141716 and SR144528, selective CB1 and CB2 receptor antagonists, were synthesized at Pfizer. The synthetic cannabinoid agonist WIN 55,212-2 and polyethyleneglycol 300 were purchased from Sigma-Aldrich (St. Louis, MO) and Fluka Analytical, respectively. Polystyrene 96- and 384-microplates were purchased from Rainin and Evergreen Scientific (Los Angeles, CA), respectively. All reagents used were the highest quality commercially available.

FAAH Expression and Purification. The hFAAH (amino acids 32-579) and rFAAH (amino acids 30-579) constructs were generated as the *N*-terminal transmembrane-deleted truncated forms with *N*-terminal His_6 tags, and were expressed in *E. coli* and purified as previously described (Mileni et al., 2008). Both hFAAH and rFAAH enzymes used in the present study had purity greater than 95% based on SDS-PAGE visualized by Coomassie blue staining. Protein concentrations were determined by using BCA protein assay kit (Pierce).

Determination of Inhibitor Potency (k_{inact}/K_i values). The glutamate dehydrogenase-coupled FAAH assay was used for determination of potencies (k_{inact}/K_i values) for the urea irreversible inhibitors. The FAAH assay was performed in 384- or 96- well microplates with a final volume

of 50 or 200 µL, respectively. The details of the assay and derivations of the overall potency, k_{inact}/K_i value, have been described previously (Mileni et al., 2008).

Determination of IC_{50} values. IC_{50} values were determined using the glutamate dehydrogenase-coupled FAAH assay by following the previously described method except with the final volume of 50 µL in 384-well microplates (Ahn et al., 2007).

In Vitro Competitive ABPP Studies. Mouse and human tissues were prepared as described previously and inhibitor selectivity was assessed using the FP-rhodamine probe by competitive activity-based protein profiling using the method as previously described (Patricelli et al., 2001; Ahn et al., 2007; Ahn et al., 2009).

Detection of Inhibitor-Labeled Proteins In Vivo using CC-ABPP. CC-ABPP studies and click chemistry reaction were performed by following previously described procedures (Alexander and Cravatt, 2005; Ahn et al., 2009). Briefly, C57BL/6 mice between the ages of 8 and 12 weeks were administered FAAH inhibitors at 10 mg/kg, i.p., in a vehicle of 18:1:1 PBS:emulphor:ethanol. After 1 hr, the mice were sacrificed by CO_2 asphyxiation. Tissue samples were harvested and immediately flash frozen in liquid nitrogen. Membrane and soluble fractions were processed from the tissue samples by dounce homogenization in PBS and subsequent centrifugation at 100,000 x g for 45 minutes at 4 ºC. These mouse tissue proteomes were diluted to yield 1 mg/ml solutions in PBS (pH 7.5). Click chemistry reaction was carried out and quenched with 50 µL of 2X SDS-PAGE loading buffer (reducing). Quenched reactions were separated by SDS-PAGE (30 µL of sample/lane) and

visualized in-gel using a Hitachi FMBio IIe flatbed laser-induced fluorescence scanner (MiraiBio, Alameda, CA).

Measurement of FAAH Activity from Rat Brain and Blood Leukocytes. The membrane fractions from the brain tissue and leukocytes were prepared and FAAH activity were measured by using ^{3}H-labeled AEA as substrate and quantifying the generated ^{3}H-labeled ethanolamine as previously described (Ahn et al., 2009).

Measurement of Lipids from Rat Brain and Plasma. Lipid levels from rat brain and plasma were measured by LC-MS using the method previously described (Ahn et al., 2009).

Experimental Animals. Male Sprague-Dawley rats were used for all in vivo efficacy experiments. Male C57BL/6J mice (Jackson Laboratories) were used to assess cannabimimetic behavior in the tetrad assay. Animal subjects had free access to food and water and were maintained on a 12/12hr light/dark cycle for the entire duration of the study. The animal colony was maintained at approximately 21 ºC and 60% humidity. All experiments were conducted in accordance with the International Association for the Study of Pain guidelines.

CFA Model of Inflammatory Pain. The detailed procedure for the CFA model has been previously described (Ahn et al., 2009). Briefly, 150 µL of CFA (1 mg/mL suspension in mineral oil, Sigma) was injected into the plantar surface of the hind paw of male Sprague-Dawley rats (200-250 g). The CFA injection immediately induces local inflammation, paw swelling, and

pain, which persist. To assess mechanical allodynia, mechanical paw withdrawal thresholds (PWTs) were measured using a set of Von Frey Hairs on day 5 postinjection as described (Dixon, 1980). PF-04457845 was administered orally to rats at the indicated dose (mg/kg) as a nanocrystalline suspension in 2% polyvinylpyrrolidone and 0.15% sodium dodecyl sulfate in H_2O in a volume of 10 mL/kg. PWTs were evaluated at 4 hr post dosing for the dose-response study or at 1, 2, 4, 8, and 24 hr post dosing for the time course study. PWT measurements were averaged and statistical comparisons between groups were made using 1 way analysis of variance (ANOVA) and Dunnett's two-tailed test.

MIA-Induced Arthritis. Unilateral osteoarthritis was induced by intra-articular injection of monosodium iodoacetate (MIA) solution in the knee joint of the rat 14 days prior to drug treatment (Bove et al., 2003; Pomonis et al., 2005). Male Sprague-Dawley rats (220-270 g) were anesthetized with isoflurane and 2 mg MIA in 0.9% saline was injected in a 50 µL volume into the synovium of the knee using a syringe with a 27 gauge needle. At day 14 after MIA injection each experimental group was orally administered at a volume of 10 mL/kg once daily for 3 consecutive days with vehicle (4% 2-hydroxypropyl-β-cyclodextran and 1% ethanol in 0.01 M HCl) or PF-04457845 (0.3 mg/kg in vehicle). celecoxib (30 mg/kg in 0.5% methylcellulose in H_2O) was dosed twice daily for 3 consecutive days. Pain was evaluated using a digital Randall-Selitto device (IITC Life Sciences, Woodland Hills, CA). Briefly, animals were allowed to acclimate to the testing room for a minimum of 30 min before testing. Baseline (pre-treatment) and post-treatment values for mechanical allodynia were assessed by placing the animal in a restraint sling that suspended the animal, leaving the hind limbs available for testing. Joint

compression thresholds were measured once at each time point for the ipsilateral and contralateral knee joints. Pressure was applied gradually over approximately 10 sec to the medial and lateral aspects of the knee joint. Measurements were taken from the first observed nocifensive behavior, including vocalization, struggle or withdrawal. A cut-off value of 500 g was used to prevent injury to the animal. The mean and standard error of the mean (SEM) were determined for each treatment group. Data were analyzed using 1-way ANOVA and Bonferroni's post-hoc tests.

Tetrad Test. Male C57BL6/J mice (7 weeks old, n = 8) were treated with PF-04457845 (1 or 10 mg/kg in polyethyleneglycol 300 vehicle by oral administration in a volume of 4 ml/kg), the synthetic cannabinoid agonist WIN 55,212-2 (1 or 10 mg/kg in 18:1:1 saline:emulphor:ethanol vehicle by intraperitoneal administration in a volume of 10 ml/kg), or the corresponding vehicle. Mice were evaluated for the hypomotility, hypothermia, antinociceptive, and cataleptic effects at 4 hr or 30 min after PF-04457845 or WIN 55,212-2 administration, respectively, using the tetrad tests (Smith et al., 1994) as previously described (Cravatt et al., 2001) except that catalepsy was assessed for 60 sec instead of 10 sec. Statistical analysis was performed using the Student's t-test comparing each treatment group to vehicle.

Results

PF-04457845 is a highly potent inhibitor of FAAH with a covalent, irreversible mechanism of action. We have recently reported our FAAH inhibitor discovery research effort culminating in the discovery of the clinical candidate PF-04457845, a benzylidenepiperidine pyridazine urea (Johnson et al., 2011) (Figure 1). Detailed mechanistic and kinetic studies, as well as X-ray crystallographic results, have revealed that this class of piperidine/piperazine urea compounds inhibit FAAH by a covalent, irreversible mechanism involving carbamylation of FAAH's catalytic Ser241 nucleophile (Ahn et al., 2007; Mileni et al., 2008; Ahn et al., 2009). The mechanism of FAAH inhibition by PF-04457845 involving the Ser241-Ser217-Lys142 catalytic triad is shown in Figure 2. The progress curves for FAAH reaction using an enzyme-coupled assay with oleamide as a substrate are shown in Figure 3. In these reactions, stoichiometric quantities of NAD^+ are formed upon generation of ammonia from oleamide by FAAH hydrolysis, which are spectrophotometrically monitored at 340 nm as described (Ahn et al., 2007). The FAAH reaction was linear for a ~40 min time period as measured by production of NAD^+ in the absence of PF-04457845 (Fig. 3A). In the presence of PF-04457845 at 5 – 625 nM, the progress curves for oleamide hydrolysis by FAAH exhibited curvature, consistent with an irreversible mechanism of inhibition. The data were fit into a pseudo-first-order decay equation to determine k_{obs} values at each inhibitor concentration. Using these k_{obs} values and the previously described derivations (Mileni et al., 2008), the potency of PF-04457845 was determined as k_{inact}/K_i values, the best measure of inhibitor potency for irreversible inhibitors. PF-04457845 displayed high in vitro potency (k_{inact}/K_i value) of 40300 ± 11000 $M^{-1}s^{-1}$ for inhibition of human FAAH (hFAAH). The potency of PF-04457845 for hFAAH inhibition was

3- and 50-fold higher compared to that of the previously reported piperidine ureas, PF-3845 and PF-750, respectively, and was 25-fold higher than that of the extensively described carbamate FAAH inhibitor URB597 (Table 1 and Figure 1). Improved potency of PF-04457845 compared to its closely related analog PF-3845 is derived from the double bond between the biphenyl ether and the piperidine moiety, and substitution of the pyridyl group with 3-aminopyridazine. These features appear to also contribute to inhibition of hFAAH and rat FAAH (rFAAH) with comparable potency unlike PF-750 and PF-3845, which inhibit hFAAH more potently than rFAAH by 3.2- and 7.6-fold, respectively (Table 1).

As expected from its irreversible inhibition, the IC_{50} values for PF-04457845 displayed time-dependence. As shown in Figure 3B and Table 2, PF-04457845 exhibited a dramatic ~7-fold increase in potency as the preincubation time with hFAAH was increased from 1 to 60 min (Table 2). With a 60-min preincubation time, PF-04457845 inhibited hFAAH with an IC_{50} value of 7.2 ± 0.63 nM. A similar time-dependent inhibition with comparable potency was also observed for inhibition of rFAAH by PF-04457845 (Figure 3C and Table 2).

PF-04457845 inhibits FAAH with exquisite in vitro and in vivo selectivity. Selectivity assessment is critical to determine whether or not any compound can serve as a potential pharmacological tool or drug. FAAH belongs to the serine hydrolase superfamily of enzymes with greater than 200 members in humans. In order to determine the in vitro selectivity of PF-04457845 against this large class of enzymes, we have profiled PF-04457845 at 10 and 100 μM by competitive activity-based protein profiling (ABPP) (Leung et al., 2003) with the serine hydrolase-directed fluorophosphonate (FP)-rhodamine probe (Patricelli et al., 2001) in multiple different proteomes derived from human and mouse sources. The selectivity of PF-04457845

was compared to that of URB597 and gel images of soluble and membrane proteomes of brain, liver, and heart from human and mouse are shown in Figure 4. We have recently reported the selectivity profile from brain membrane and soluble liver proteomes of human and mouse(Johnson et al., 2011), which was also included in Figure 4 for comparison. Both PF-04457845 and URB597 completely inhibited FAAH in brain membrane proteomes from human and mouse at both 10 and 100 μM with no off targets (Figure 4A). However, in other proteomes, the profiles of PF-04457845 were drastically different than those of URB597. PF-04457845 was completely selective for FAAH as none of the other FP-reactive serine hydrolases in the tested tissues were inhibited by PF-04457845 even at 100 μM. In contrast, URB597 blocked the FP labeling of several serine hydrolases at 10 μM in addition to FAAH, particularly between 55 and 65 kDa in soluble proteomes of brain, liver, and heart in addition to membrane proteomes of liver from human and mouse sources (Figure 4B, C, and D). It is noteworthy that URB597, which has been reported to be highly selective for serine hydrolases in mouse brain proteomes, inhibits at least one additional serine hydrolase in soluble proteomes of human brain migrating at ~60 kDa, which was completely inhibited by URB597 at 10 μM (Figure 4C). In soluble proteome of mouse brain, URB597 appears to be completely selective at 10 μM while inhibiting several off targets migrating at ~66-80 kDa at 100 μM (Figure 4D). These data indicate that URB597 at 10 μM is completely selective in soluble brain proteome from mouse but not from human. We have previously determined that several of these URB597 off-targets in the soluble proteome of mouse liver (which were inhibited with IC_{50} values well below 1 μM) are carboxyesterases (Alexander and Cravatt, 2005; Ahn et al., 2007). PF-04457845 at 100 μM was

also profiled by ABPP in several additional proteomes including kidney, spleen, and testis, and found to be completely selective (data not shown).

We have also recently reported that PF-04457845 at 10 μM displayed a highly favorable selectivity profile against a broad panel of 68 targets including receptors, enzymes, ion channels, and transporters (Johnson et al., 2011).

Next, in order to more broadly assess the selectivity of PF-04457845 in vivo, we synthesized an alkyne derivative of PF-04457845, termed PF-04457845yne (Figure 5A). Replacement of the trifluoromethyl substituent in PF-04457845 with a pentynyloxy group resulted in PF-04457845yne (Figure 5A), which maintained high potency for FAAH (k_{inact}/K_i value of 11900 ± 1900 $M^{-1}s^{-1}$). We then applied click chemistry (CC)-ABPP for direct analysis of the protein targets that are covalently modified by PF-04457845yne in vivo (Speers et al., 2003; Alexander and Cravatt, 2005; Ahn et al., 2009). In this approach, tissues isolated from animals after treatment with PF-04457845yne are reacted with a rhodamine-azide tag under CC conditions to yield the corresponding triazole product, and labeled proteins are visualized by in-gel fluorescence scanning (Figure 5B and C). As in the in vitro selectivity assessment, we compared the selectivity profile of PF-04457845yne with that of JP104, an alkyne derivative of URB597 (Alexander and Cravatt, 2005). Mice were treated with PF-04457845yne and JP104 (10 mg/kg, intraperitoneal (i.p.)) for 2 hr and the animals were sacrificed. The labeled proteins in brain and liver proteomes were analyzed by CC-ABPP using a rhodamine-azide tag. As shown in Figure 5B, both PF-04457845yne and JP104 selectively reacted with a single target in mouse brain which was confirmed to be FAAH as this band is absent in FAAH(-/-) mice. PF-04457845yne also selectively reacted with FAAH in liver (Figure 5C). In contrast, JP104 reacted with several

targets that are present in both FAAH(+/+) and FAAH(-/-) mice, as reported previously (Alexander and Cravatt, 2005; Ahn et al., 2009). A single faint band at ~60 kDa in liver proteomes was labeled even in vehicles of both FAAH(+/+) and FAAH(-/-) mice representing a nonspecific target of the rhodamine-azide tag. Taken together, these ABPP data indicate that PF-04457845 displays exquisite in vitro and in vivo selectivity for FAAH.

Pharmacokinetic characterization. PF-04457845 has high oral bioavailability of 88% and 58% in rat and dog, respectively (Johnson et al., 2011). The plasma and brain concentrations of PF-04457845 reached peak levels of 246 ng/mL (540 nM) and 396 ng/g tissue (870 nM) at 4 hr after oral administration at 1 mg/kg in rats (Figure 6), indicating that PF-04457845 has high brain permeability with a concentration ratio of 1.6 for brain versus plasma. The maximum plasma concentration of PF-04457845 after oral administration at 5 mg/kg in rats was 1270 ng/mL (2.8 μM) (t_{max} = 2 hr) indicating that the plasma concentrations of PF-04457845 is highly linear between 1 and 5 mg/kg (p.o).

PF-04457845 displays anti-hyperalgesic activity in a rodent model of inflammatory pain, which coincides with dramatic and sustained elevations in AEA and other NAEs. We assessed PF-04457845 in a rat model of CFA-induced inflammatory pain, which we have recently described (Johnson et al., 2011). Our objective in the present study was to determine the relationship between the in vivo efficacy and modulation of FAAH activity and substrate levels (i.e., NAEs) by PF-04457845 in central (brain) and peripheral systems (peripheral blood leukocytes/plasma). For this purpose, the CFA efficacy data are presented here side-by-side with the FAAH activity and substrate levels. PF-04457845 orally administered at 0.003-10 mg/kg displayed statistically significant inhibition of mechanical allodynia at a dose as low as 0.1

mg/kg to a comparable degree as the nonsteroidal anti-inflammatory drug naproxen at 10 mg/kg (p.o.) (Figure 7A). As shown in Figure 7B and 7C, robust, near-complete inhibition of FAAH activity with concomitant elevations in AEA was observed in brain and peripheral blood leukocytes/plasma from PF-04457845-treated animals at all efficacious doses (Figure 7B and 7C). AEA was elevated by 5-7-fold in brain of the PF-04457845-treated animals at the efficacious doses. In plasma, AEA was elevated to a lower extent (3-5-fold) compared to brain (Figure 7C). Furthermore, OEA and PEA were also elevated by 8-20-fold in brain at the efficacious doses (Figure 7D). It is noteworthy that near-complete FAAH inhibition (greater than 98%) was observed in brain and blood leukocytes at all efficacious doses (greater than 0.1 mg/kg). Importantly, NAE levels from brain and plasma were elevated to their near maximal levels at a minimum effective dose of 0.1 mg/kg and were maintained at the maximal levels at higher doses (0.3-10 mg/kg) (Figure 7C and 7D). These data indicate that near complete inhibition of FAAH activity and maximal sustained elevation of AEA correlate with in vivo efficacy in the CFA model, which is in full agreement with previous observations (Ahn et al., 2009). These data could also explain why a sharp dose response was observed in the CFA model and the extent of pain inhibition by PF-04457845 was similar at all efficacious doses, as near-complete inhibition of FAAH activity and maximal elevation of AEA correlate with in vivo efficacy. These could also be explained by a covalent, irreversible inhibition of PF-04457845. Once all FAAH has been fully inactivated by covalent formation with PF-04457845, the excess compound levels at higher doses do not lead to any greater efficacy. Naproxen did not show FAAH inhibition or AEA and other NAE modulation (Figure 7B, C, and D) indicating that the in vivo efficacy mediated by this compound is not due to FAAH inhibition.

The high in vivo potency of PF-04457845 is evident by the low compound exposure levels at efficacious doses in the CFA model as shown in Figure 7E. At the minimum effective dose of 0.1 mg/kg, the exposure levels of PF-04457845 were as low as 17.7 ng/g brain tissue (38.9 nM) and 15.8 ng/ml plasma (34.7 nM). These low compound concentrations in plasma and brain were sufficient to provide maximal in vivo efficacy, near complete inhibition of FAAH activity (Figure 7B), and full modulation of AEA and other NAEs (Figure 7C and 7D). These results illustrate a benefit of the irreversible mechanism of inhibition by PF-04457845. PF-04457845 showed comparable exposure levels in brain tissue and plasma (Average Brain/Plasma = ~1.3) at all efficacious doses, again indicating that this compound has excellent brain penetration.

PF-04457845 produces a long duration of action in the CFA model and its anti-hyperalgesic effect is cannabinoid receptor-dependent. We next evaluated the duration of action of PF-04457845 in the CFA model from 1-24 hr post-administration. A single oral administration of PF-04457845 at 1 mg/kg produced significant inhibition of mechanical allodynia at all time points up to 24 hr (Figure 8A). As expected, near complete inhibition of FAAH activity and maximal elevations of AEA were observed both in brain and plasma (Figure 8B and 8C). It is noteworthy that the extent of elevation for AEA (5-7-fold) in brain was greater than that in plasma (3-5-fold). PEA and OEA were also greatly elevated in brain (8-13-fold) (Figure 8D) and to a lesser extent in plasma (data not shown), similar to what was observed with efficacious doses of a related FAAH inhibitor, PF-3845 (Ahn et al., 2009).

We further examined involvement of cannabinoid receptors in the PF-04457845-induced antiallodynia using selective antagonists for central CB1 (SR141716) and peripheral CB2 (SR144528) receptors. As shown in Figure 8E, CB1 and CB2 antagonists each only partially

reduced the antiallodynia activity of PF-044578945, while treatment with a combination of CB1 and CB2 antagonists produced a near complete abolishment of the PF-04457845-induced anti-hyperalgesia in the CFA model (Figure 8E). These data indicate that PF-04457845 inhibits inflammatory pain responses in the CFA model by a cannabinoid receptor-dependent mechanism that involve both CB1 and CB2 receptors, as previously shown for other FAAH inhibitors such as PF-3845 (Ahn et al., 2009) and URB597 (Jayamanne et al., 2006). As expected, the CB1 or CB2 antagonist alone had no effect on mechanical allodynia (Figure 8E).

PF-04457845 exhibits an anti-hyperalgesic effect in a chronic noninflammatory pain model. Next we assessed PF-04457845 in a rat noninflammatory chronic arthritic pain model (monosodium iodoacetate (MIA)-induced arthritis model) at 0.3 and 3 mg/kg, doses at which near complete inhibition of FAAH activity and maximal sustained elevation of AEA were observed in rats as shown above (Figure 8). Intra-articular injection of MIA resulted in the development of significant and prolonged osteoarthritis-related pain as displayed by an increase in primary mechanical hyperalgesia compared to naïve animals at 14 days after MIA injection. As shown in Figure 9A, joint compression thresholds at pre-dosing baseline in the ipsilateral knees were significantly reduced compared to the contralateral knees as illustrated by dotted line (105 g compared to 400 g) demonstrating the hypersensitivity induced in this model. Oral administration of PF-04457845 at 0.3 and 3 mg/kg once daily for 3 consecutive days significantly increased joint compression thresholds at 2 and 4 hr after administration compared to vehicle-treated animals (Figure 9A, Day 3). The extent of pain inhibition by PF-04457845 was comparable to that of a selective cycloxygenase 2 (COX2) inhibitor celecoxib dosed at 30 mg/kg (p.o.) twice per day for 3 consecutive days (Figure 9A, Day 3). Even a single day treatment with

PF-04457845 effectively increased joint compression thresholds. PF-04457845 at 3 mg/kg (p.o.) significantly reduced mechanical allodynia compared to vehicle-treated animals both 2 and 4 hr after administration on day 1 (Figure 9A, Day 1). As observed in the CFA model, PF-04457845 administered at both 0.3 and 3 mg/kg (p.o.) yielded comparable efficacy in most cases as both doses are expected to produce complete inhibition of FAAH that is needed to generate sustained maximal level of AEA for efficacy. As shown in Figure 9B, PF-04457845 or celecoxib had no effect on the pain behavior in noninjured knee (i.e., contralateral knee joint) as expected.

PF-04457845 elicits no effect in motility, catalepsy and body temperature. In order to evaluate whether PF-04457845 produces any undesirable side effects typically associated with direct CB1 agonists, we assessed mice treated with PF-04457845 at 1 and 10 mg/kg (p.o.). The doses of 1 and 10 mg/kg are chosen for this study as they are 10- and 100-fold higher than the minimum effective dose of 0.1 mg/kg, respectively, where FAAH was shown to be completely inhibited as discussed above in the CFA study. We have assessed PF-04457845 in the "tetrad test" for cannabinoid behavior, consisting of assays for antinociception, catalepsy, hypomotility, and hypothermia (Smith et al., 1994). We also assessed the cannabinoid agonist WIN 55,212-2 in the tetrad test for comparison. PF-04457845 orally administered at 1 and 10 mg/kg caused antinociceptive effects in the thermal tail immersion test at 4 hr post-dosing (Figure 10B), with increased tail withdrawal latencies over vehicle, which were comparable to those observed previously following pharmacological or genetic FAAH inactivation (Cravatt et al., 2001; Long et al., 2009). Neither doses of PF-04457845 elicited any effect in locomotive activity, catalepsy or body temperature (Figure 10A, C, and D). In contrast, significant cannabinoid behavioral

effects were observed following treatment with 10 mg/kg WIN 55,212-2 (i.p.) at 30 min post-dosing as expected from a direct CB1 agonist (Figure 10A-D). As expected, FAAH was confirmed to be completely inhibited in mice treated with PF-04457845 at 1 and 10 mg/kg (p.o.) by competitive ABPP as shown in Supplemental Figure 1.

Discussion

The pharmacological blockade of FAAH has emerged as a potentially attractive strategy by which to elevate endocannabinoid signaling and retain the beneficial effects of cannabinoid receptor activation, while avoiding the undesirable effects of global cannabinoid receptor activation. Over the past decade, there have been tremendous advances in the development of FAAH inhibitors. Several classes of FAAH inhibitors that vary in their mechanism of action, potency, selectivity, and in vivo efficacy have been described. In order to develop a FAAH inhibitor as a clinical candidate, identification of an agent that displays an optimal combination of efficacy and selectivity, as well as suitable pharmacokinetic properties for human dosing is required. We have described herein the detailed characterization of the clinical candidate PF-04457845, a benzylidenepiperidine pyridazine urea FAAH inhibitor that satisfies these criteria. PF-04457845 has a high in vitro potency for hFAAH inhibition that is 3- and 50-fold higher compared to the potencies of previously reported piperidine ureas, PF-3845 and PF-750, respectively, and is 25-fold higher than that of the most extensively described carbamate FAAH inhibitor URB597 (Table 1 and Figure 1). PF-04457845 also inhibits both hFAAH and rFAAH with equivalent potency unlike PF-750 and PF-3845, which inhibit hFAAH more potently than rFAAH, by 3.2 and 7.6-fold, respectively (Table 1), ABPP experiments indicate that PF-04457845 displays exquisite selectivity for FAAH both in vitro and in vivo (Figures 4 and 5). PF-04457845 exhibits remarkable in vivo activity, which is reflected in sustained inhibition of brain FAAH activity and maximal elevations of brain AEA with an oral administration dose as low as 0.1 mg/kg that correlate with cannabinoid receptor-dependent reductions in inflammatory pain responses (Figure 7 and 8). PF-04457845 has excellent pharmaceutical properties as evident

from high oral bioavailability of 88% in rats, high brain penetration (ratio of 1.3-1.6 for brain versus plasma concentrations) (Figure 6), and long duration of action where a single oral administration of PF-04457845 at 1 mg/kg exhibited in vivo efficacy in the CFA model for at least 24 hr (Figure 8).

In addition to providing data showing robust in vivo efficacy for PF-04457845 in a rat model of inflammatory pain (CFA model) (Figure 7 and 8), we also assessed the efficacy of PF-04457845 in a noninflammatory osteoarthritis-like MIA pain model. In the acute phase of this model (days 1-3), inflammatory pathology with limited structural disorder is known to appear after MIA injection to the knee joint. In the chronic phase (days 14-28), inflammation is reduced, and severe morphological disorders similar to OA joints are detected (Bove et al., 2003; Pomonis et al., 2005). In this MIA model, PF-04457845 showed significantly reduced mechanical hyperalgesia following even a single dose of treatment. The level of analgesia observed was comparable to that of the selective COX2 inhibitor celecoxib (Figure 9).

Furthermore, we reported that PF-04457845 administered at doses that are 10-100-fold higher than the minimum effective in vivo efficacy dose displayed no effect in motility, catalepsy, and body temperature. Significantly, we also showed a tight relationship between in vivo efficacy and FAAH activity/AEA modulation in brain and leukocytes/plasma where near complete inhibition of FAAH and a maximal sustained elevation of AEA appear to be needed for in vivo efficacy (Figure 7-8). The ability to measure both FAAH activity and AEA levels from blood leukocytes and plasma, respectively, provides potentially valuable mechanistic biomarkers for human clinical studies.

In summary, we report the mechanistic and pharmacological characterization of PF-04457845, a piperidine urea FAAH inhibitor that combines high target selectivity with exceptional in vivo efficacy and pharmacokinetic properties. PF-04457845 was shown to covalently inactivate FAAH by carbamylation of the enzyme's active site Ser241 nucleophile. PF-04457845 completely inhibits FAAH without reacting with other serine hydrolases in vivo as determined by competitive ABPP and possesses a long duration of action reflected in sustained in vivo efficacy for at least 24 hr after a single oral administration at 1 mg/kg. PF-04457845 displays robust efficacy in rat models of both acute inflammatory and chronic noninflammatory pain. PF-04457845 elicits no effects in motility, catalepsy, and body temperature. Based on these data, PF-04457845 has been selected as a clinical candidate for the treatment of pain and other central nervous system disorders.

Acknowledgments

We thank Udeni Yapa for measuring drug exposure levels.

Authorship Contributions

Participated in research design: Ahn, Beidler, Sadagopan, Dudley, Young, Wren, Johnson, and Cravatt

Conducted experiments: Smith, Liimatta, Zhang, Swaney, Van Becelaere, Blankman, Nomura, Bhattachar, Nomanbhoy, Weerapana,

Contributed new reagents or analytical tools: Stiff, Johnson

Performed data analysis: Ahn, Smith, Liimatta, Sadagopan, Zhang, Swaney, Van Becelaere, Blankman, Nomura

Wrote or contributed to the writing of the manuscript: Ahn, Cravatt

References

Ahn K, Johnson DS, Fitzgerald LR, Liimatta M, Arendse A, Stevenson T, Lund ET, Nugent RA, Nomanbhoy TK, Alexander JP and Cravatt BF (2007) Novel mechanistic class of fatty acid amide hydrolase inhibitors with remarkable selectivity. *Biochemistry* **46**:13019-13030.

Ahn K, Johnson DS, Mileni M, Beidler D, Long JZ, McKinney MK, Weerapana E, Sadagopan N, Liimatta M, Smith SE, Lazerwith S, Stiff C, Kamtekar S, Bhattacharya K, Zhang Y, Swaney S, Van Becelaere K, Stevens RC and Cravatt BF (2009) Discovery and characterization of a highly selective FAAH inhibitor that reduces inflammatory pain. *Chem Biol* **16**:411-420.

Ahn K, McKinney MK and Cravatt BF (2008) Enzymatic pathways that regulate endocannabinoid signaling in the nervous system. *Chem Rev* **108**:1687-1707.

Alexander JP and Cravatt BF (2005) Mechanism of carbamate inactivation of FAAH: implications for the design of covalent inhibitors and in vivo functional probes for enzymes. *Chem Biol* **12**:1179-1187.

Boger DL, Miyauchi H, Du W, Hardouin C, Fecik RA, Cheng H, Hwang I, Hedrick MP, Leung D, Acevedo O, Guimaraes CR, Jorgensen WL and Cravatt BF (2005) Discovery of a potent, selective, and efficacious class of reversible alpha-ketoheterocycle inhibitors of fatty acid amide hydrolase effective as analgesics. *J Med Chem* **48**:1849-1856.

Bove SE, Calcaterra SL, Brooker RM, Huber CM, Guzman RE, Juneau PL, Schrier DJ and Kilgore KS (2003) Weight bearing as a measure of disease progression and efficacy of anti-inflammatory compounds in a model of monosodium iodoacetate-induced osteoarthritis. *Osteoarthritis Cartilage* **11**:821-830.

Chang L, Luo L, Palmer JA, Sutton S, Wilson SJ, Barbier AJ, Breitenbucher JG, Chaplan SR and Webb M (2006) Inhibition of fatty acid amide hydrolase produces analgesia by multiple mechanisms. *Br J Pharmacol* **148**:102-113.

Cravatt BF, Demarest K, Patricelli MP, Bracey MH, Giang DK, Martin BR and Lichtman AH (2001) Supersensitivity to anandamide and enhanced endogenous cannabinoid signaling in mice lacking fatty acid amide hydrolase. *Proc Natl Acad Sci U S A* **98**:9371-9376.

Cravatt BF, Giang DK, Mayfield SP, Boger DL, Lerner RA and Gilula NB (1996) Molecular characterization of an enzyme that degrades neuromodulatory fatty-acid amides. *Nature* **384**:83-87.

Cravatt BF, Prospero-Garcia O, Siuzdak G, Gilula NB, Henriksen SJ, Boger DL and Lerner RA (1995) Chemical characterization of a family of brain lipids that induce sleep. *Science* **268**:1506-1509.

Cravatt BF, Saghatelian A, Hawkins EG, Clement AB, Bracey MH and Lichtman AH (2004) Functional disassociation of the central and peripheral fatty acid amide signaling systems. *Proc Natl Acad Sci U S A* **101**:10821-10826.

Dixon WJ (1980) Efficient analysis of experimental observations. *Annu Rev Pharmacol Toxicol* **20**:441-462.

Gobbi G, Bambico FR, Mangieri R, Bortolato M, Campolongo P, Solinas M, Cassano T, Morgese MG, Debonnel G, Duranti A, Tontini A, Tarzia G, Mor M, Trezza V, Goldberg SR, Cuomo V and Piomelli D (2005) Antidepressant-like activity and modulation of brain monoaminergic transmission by blockade of anandamide hydrolysis. *Proc Natl Acad Sci U S A* **102**:18620-18625.

Holt S, Comelli F, Costa B and Fowler CJ (2005) Inhibitors of fatty acid amide hydrolase reduce carrageenan-induced hind paw inflammation in pentobarbital-treated mice: comparison with indomethacin and possible involvement of cannabinoid receptors. *Br J Pharmacol* **146**:467-476.

Huitron-Resendiz S, Sanchez-Alavez M, Wills DN, Cravatt BF and Henriksen SJ (2004) Characterization of the sleep-wake patterns in mice lacking fatty acid amide hydrolase. *Sleep* **27**:857-865.

Jayamanne A, Greenwood R, Mitchell VA, Aslan S, Piomelli D and Vaughan CW (2006) Actions of the FAAH inhibitor URB597 in neuropathic and inflammatory chronic pain models. *Br J Pharmacol* **147**:281-288.

Johnson D, Stiff C, Lazerwith S, Kesten S, Fay L, Morris M, Beidler D, Liimatta M, Smith S, Dudley D, Sadagopan N, Bhattachar S, Kesten S, Nomanbhoy T, Cravatt B and Ahn K (2011) Discovery of PF-04457845: A Highly Potent, Orally Bioavailable, and Selective Urea FAAH Inhibitor. *ACS Med Chem Lett* **2(2)**:91-96.

Johnson DS, Ahn K, Kesten S, Lazerwith SE, Song Y, Morris M, Fay L, Gregory T, Stiff C, Dunbar JB, Jr., Liimatta M, Beidler D, Smith S, Nomanbhoy TK and Cravatt BF (2009) Benzothiophene piperazine and piperidine urea inhibitors of fatty acid amide hydrolase (FAAH). *Bioorg Med Chem Lett* **19**:2865-2869.

Kathuria S, Gaetani S, Fegley D, Valino F, Duranti A, Tontini A, Mor M, Tarzia G, La Rana G, Calignano A, Giustino A, Tattoli M, Palmery M, Cuomo V and Piomelli D (2003) Modulation of anxiety through blockade of anandamide hydrolysis. *Nat Med* **9**:76-81.

Kinsey SG, Long JZ, O'Neal ST, Abdullah RA, Poklis JL, Boger DL, Cravatt BF and Lichtman AH (2009) Blockade of endocannabinoid-degrading enzymes attenuates neuropathic pain. *J Pharmacol Exp Ther* **330**:902-910.

Kinsey SG, O'Neal ST, Long JZ, Cravatt BF and Lichtman AH (2010) Inhibition of endocannabinoid catabolic enzymes elicits anxiolytic-like effects in the marble burying assay. *Pharmacol Biochem Behav*.

Lambert DM, Vandevoorde S, Jonsson KO and Fowler CJ (2002) The palmitoylethanolamide family: a new class of anti-inflammatory agents? *Curr Med Chem* **9**:663-674.

Leung D, Hardouin C, Boger DL and Cravatt BF (2003) Discovering potent and selective reversible inhibitors of enzymes in complex proteomes. *Nat Biotechnol* **21**:687-691.

Lichtman AH, Leung D, Shelton CC, Saghatelian A, Hardouin C, Boger DL and Cravatt BF (2004) Reversible inhibitors of fatty acid amide hydrolase that promote analgesia: evidence for an unprecedented combination of potency and selectivity. *J Pharmacol Exp Ther* **311**:441-448.

Long JZ, Nomura DK, Vann RE, Walentiny DM, Booker L, Jin X, Burston JJ, Sim-Selley LJ, Lichtman AH, Wiley JL and Cravatt BF (2009) Dual blockade of FAAH and MAGL identifies behavioral processes regulated by endocannabinoid crosstalk in vivo. *Proc Natl Acad Sci U S A* **106**:20270-20275.

Massa F, Marsicano G, Hermann H, Cannich A, Monory K, Cravatt BF, Ferri G-L, Sibaev A, Storr M and Lutz B (2004) The endogenous cannabinoid system protects against colonic inflammation. *J Clin Invest* **113**:1202-1209.

McKinney MK and Cravatt BF (2003) Evidence for distinct roles in catalysis for residues of the serine-serine-lysine catalytic triad of fatty acid amide hydrolase. *J Biol Chem* **278**:37393-37399.

McKinney MK and Cravatt BF (2005) Structure and function of fatty acid amide hydrolase. *Annu Rev Biochem* **74**:411-432.

Mechoulam R (1986) The Pharmacohistory of *Cannabis sativa* (Boca Raton, FL: CRS Press). in.

Mileni M, Garfunkle J, DeMartino JK, Cravatt BF, Boger DL and Stevens RC (2009) Binding and inactivation mechanism of a humanized fatty acid amide hydrolase by alpha-ketoheterocycle inhibitors revealed from cocrystal structures. *J Am Chem Soc* **131**:10497-10506.

Mileni M, Johnson DS, Wang Z, Everdeen DS, Liimatta M, Pabst B, Bhattacharya K, Nugent RA, Kamtekar S, Cravatt BF, Ahn K and Stevens RC (2008) Structure-guided inhibitor design for human FAAH by interspecies active site conversion. *Proc Natl Acad Sci USA* **105**:12820-12824.

Naidu PS, Kinsey SG, Guo TL, Cravatt BF and Lichtman AH (2010) Regulation of inflammatory pain by inhibition of fatty acid amide hydrolase. *J Pharmacol Exp Ther* **334**:182-190.

Naidu PS, Varvel SA, Ahn K, Cravatt BF, Martin BR and Lichtman AH (2007) Evaluation of fatty acid amide hydrolase inhibition in murine models of emotionality. *Psychopharmacology (Berl)* **192**:61-70.

Patricelli MP, Giang DK, Stamp LM and Burbaum JJ (2001) Direct visualization of serine hydrolase activities in complex proteomes using fluorescent active site-directed probes. *Proteomics* **1**:1067-1071.

Patricelli MP, Lovato MA and Cravatt BF (1999) Chemical and mutagenic investigations of fatty acid amide hydrolase: evidence for a family of serine hydrolases with distinct catalytic properties. *Biochemistry* **38**:9804-9812.

Pomonis JD, Boulet JM, Gottshall SL, Phillips S, Sellers R, Bunton T and Walker K (2005) Development and pharmacological characterization of a rat model of osteoarthritis pain. *Pain* **114**:339-346.

Rodriguez de Fonseca F, Navarro M, Gomez R, Escuredo L, Nava F, Fu J, Murillo-Rodriguez E, Giuffrida A, LoVerme J, Gaetani S, Kathuria S, Gall C and Piomelli D (2001) An anorexic lipid mediator regulated by feeding. *Nature* **414**:209-212.

Russo R, Loverme J, La Rana G, Compton TR, Parrott J, Duranti A, Tontini A, Mor M, Tarzia G, Calignano A and Piomelli D (2007) The fatty acid amide hydrolase inhibitor URB597 (cyclohexylcarbamic acid 3'-carbamoylbiphenyl-3-yl ester) reduces neuropathic pain after oral administration in mice. *J Pharmacol Exp Ther* **322**:236-242.

Smith PB, Compton DR, Welch SP, Razdan RK, Mechoulam R and Martin BR (1994) The pharmacological activity of anandamide, a putative endogenous cannabinoid, in mice. *J Pharmacol Exp Ther* **270**:219-227.

Speers AE, Adam GC and Cravatt BF (2003) Activity-based protein profiling in vivo using a copper(i)-catalyzed azide-alkyne [3 + 2] cycloaddition. *J Am Chem Soc* **125**:4686-4687.

Footnotes

This work was supported by Pfizer Worldwide Research and Development and also in part by the NIH (DA017259, B.F.C.; F31 DA026261, J.L.B.; K99DA030908, D.K.N.) and a Pfizer Postdoctoral Fellowship (E.W.).

Send reprint requests to:

Dr. Kay Ahn

Worldwide Pfizer Research and Development

Mail Box 8220-3345

Eastern Point Road

Groton, CT 06340

E-mail: kay.ahn@pfizer.com

Legends for figures

Figure 1. Structures of PF-04457845 and other FAAH inhibitors.

Figure 2. Mechanism of covalent, irreversible inhibition of FAAH by PF-04457845. The catalytic triad Ser241-Ser217-Lys142 is shown.

Figure 3. (A) Progress curves for inhibition of human FAAH by PF-04457845 in the presence (5-625 nM) or absence of PF-04457845. (B-C) FAAH inhibition by PF-04457845 is time-dependent. Initial rates were determined using a microplate reader as described under Methods. The concentrations of PF-04457845 were varied from 1 nM to 10 μM. Three separate experiments were performed and the averages ± SD were plotted as percentage of control versus inhibitor concentration and fit to the equation, $y = 100/ [1 + (x/\mathrm{IC50})^z]$, using KaleidaGraph (Synergy Software, Reading, PA), where IC_{50} is the inhibitor concentration at 50% inhibition and z is the Hill slope (the slope of the curve at its inflection point). The IC_{50} curves are shown for inhibition of human FAAH (B) and rat FAAH (C) with preincubation times of 1, 5, 30, and 60 min.

Figure 4. Selectivity profiling of PF-04457845 and URB597 by competitive ABPP. Gel images of proteomes labeled with FP-rhodamine in the presence or absence of FAAH inhibitors (lane 1, DMSO; lane 2, URB597 at 100 μM; lane 3, URB597 at 10 μM; lane 4, PF-04457845 at 100 μM; lane 5, PF-04457845 at 10 μM; lane 6, DMSO). Gel profiles of FP-rhodamine-labeled membrane serine hydrolases from mouse and human in (A) brain and (B) liver in the presence or absence of PF-04457845 and URB597. Gel profiles of FP-rhodamine-labeled soluble serine hydrolases in brain, liver, and heart from (C) human and (D) mouse in the presence or absence of PF-

04457845 and URB597. The band on the gel corresponding to the FAAH enzyme is highlighted by the black arrow. Note that URB597, not PF-04457845, blocks FP-rhodamine labeling of several soluble serine hydroases from liver and heart as well as membrane hydrolases from liver (red arrows and brackets). In all cases, fluorescent gel images are shown in grayscale.

Figure 5. Assessment of in vivo protein targets of alkyne analogs of PF-04457845 and URB597 by CC-ABPP. (A) Structures of PF-04457845yne and JP104, alkyne analogs of PF-04457845 and URB597, respectively. (B and C) Gel profiles of CC-ABPP studies; (B) Brain or (C) liver mice proteomes were isolated after treatment with PF-04457845yne and JP104 for 2 hr at 10 mg/kg (i.p.), reacted with a rhodamine-azide tag under CC conditions, and analyzed in-gel fluorescent scanning (shown in grayscale). PF-04457845yne selectively labels FAAH in both brain and liver tissues as shown ~60kDa band is absent in FAAH(-/-) mice), which is in contrast to JP104 which labels several additional proteins in liver (protein bands present in both FAAH(+/+) and FAAH(-/-) mice). Note that the 55kDa protein band observed in liver proteome from PF-04457845yne-treated FAAH(-/-) mice was also detected in liver proteomes from vehicle-treated FAAH(+/+) and (-/-) mice and therefore most likely represents a background protein that cross-reacts with the azide-rhodamine tag.

Figure 6. Pharmacokinetic profile of PF-04457845 in rats. After oral administration of PF-04457845 at 1 mg/kg, plasma (ng/ml) or brain (ng/g tissue) concentrations of PF-04457845 were measured at 1, 2, 4, 8, and 24 hr.

Figure 7. Antihyperalgesic effects of PF-04457845 in the CFA model of inflammatory pain in rats.(A) PF-04457845 at 0.003-10 mg/kg (p.o.) produces a reduction of mechanical allodynia (hyperalgesia) (black bars). The effect of the nonsteroidal antiinflammatroy drug naproxen (10 mg/kg, p.o., hatched bar) is shown for comparison. PWTs were measured at 4 hr following drug treatment and were significantly different for PF-04457845 (0.1-10 mg/kg) and naproxen as compared to vehicle-treated groups. ***p<0.001, n = 8 rats/group. (B and D) PF-04457845-treated rats at 0.1-10 mg/kg show (B) near complete inhibition of FAAH activity and (C) elevated AEA levels in brain tissue and blood leukocytes/plasma, and (D) elevated PEA/OEA levels in brain tissue. All FAAH activity and NAE measurements were determined at 4 hr after drug treatment and were significantly different between PF-0457845- and vehicle-treated groups (p < 0.001 for FAAH activity, p < 0.01 for NAEs, n = 3 rats/group). (E) Brain and plasma levels of PF-04457845 measured at 4 hr after drug treatment. n = 3 rats/group. All data are expressed as means ± SEM.

Figure 8. Time course for antihyperalgesic effects of PF-04457845 (1 mg/kg, p.o.) in the CFA model of inflammatory pain in rats. All data are expressed as means ± SEM. (A) A single dose treatment of PF-04457845 (1 mg/kg, po) produces a reduction of mechanical allodynia at least for 24 hr. ***p<0.001, 11 rats per group. (B-D) At 1, 2, 4, 8, and 24 hr after treatment with PF-04457845, (B) near complete inhibition of FAAH activity and (C) elevated AEA levels in brain tissue and blood leukocytes/plasma, and (D) elevated PEA/OEA levels in brain tissue. All FAAH activity and NAE measurements were determined at the indicated times after drug treatment and were significantly different between PF-04457845- and vehicle-treated groups (p < 0.001. n = 3 rats/group). (E) Blockade of anti-hyperalgesic effects of PF-04457845 (3 mg/kg, p.o.) by CB1

and CB2 antagonists (SR141716 and SR144528, respectively; 3 mg/kg, i.p., each administered 10 min prior to measurement of PWTs). Note that neither the CB1 nor CB2 antagonist displayed significant effects on mechanical allodynia in rats not treated with PF-04457845 (hatched bars). $^{\#}p<0.01$, for PF-04457845- versus vehicle-treated groups. $^{**}p < 0.01$, for vehicle-PF-04457845 versus CB1/CB2 antagonist-PF-04457845 treated groups. n = 8 rats/group.

Figure 9. Antihyperalgesic effects of PF-04457845 in the MIA model of noninflammatory pain in rats. At 14 days post-MIA injection, primary mechanical hyperalgesia of the ipsilateral knees is observed (Pre-dosing baseline, Day 1) as shown by a decreases in the joint compression threshold compared to contralateral values (average contralateral values for vehicle-treated rats are illustrated by dotted line at 400 ± 14 g, n= 10). (A) PF-04457845 at 0.3 and 3 mg/kg (p.o.) once daily for 3 consecutive days produces a reduction of mechanical allodynia (hyperalgesia) at 2 and 4 hr following drug treatment on both day 1 and day 3 (grey bars for 0.3 mg/kg and black bars for 3 mg/kg). All but 0.3 mg/kg-treated rats at 4 hr on day 1 were statistically significant as compared to vehicle-treated groups. The effect of the treatment with the COX2 inhibitor celecoxib (30 mg/kg, p.o.) twice daily for 3 consecutive days (hatched bars) is shown for comparison. Joint compression thresholds were measured at 2 and 4 hr postadministration of drug treatment after 14 days following MIA injection on day 1 and day 3. (B) Joint compression thresholds were measured in the hind knee joint contralateral to injury by MIA injection. Inhibitor treatment does not affect pain behavior in the contralateral knee joint. $^{*}p<0.05$, $^{**}p<0.01$, $^{***}p<0.001$, n = 10 rats/group. Data are expressed as means ± SEM.

Figure 10. Assessment of cannabinoid behaviors of PF-04457845 in mice. Mice treated with PF-04457845 (1 and 10 mg/kg, p.o.) at 4 hr post-dosing were subjected to behavioral testing for

cannabinoid phenotypes, termed the "tetrad test", which includes assessment of (A) locomotive activity, (B) thermal nociception using a tail-immersion test, (C) catalepsy, and (D) body temperature. Mice were also treated with WIN55212-2 (WIN) (1 and 10 mg/kg, i.p.) and behavioral analysis were performed 30 min post-dosing. As expected, a cannabinoid receptor agonist WIN55212-2 caused full cannabinoid behaviors (i.e. hypomotility, thermal anti-nociception, catalepsy, and hypothermia. In contrast, PF-04457845 elicited no effect in locomotive activity, catalepsy, and body temperature while displaying significant antinociceptive effects in the thermal tail immersion test. Data are presented as average ± SEM, n=8 mice/group. **p<0.01, ***p<0.001 for treatment groups versus their respective vehicle controls.

Tables

Table 1. **Human and rat FAAH inhibition potency (k_{inact}/K_i values) of various FAAH inhibitors[a].**

Inhibitor	k_{inact}/K_i ($M^{-1}s^{-1}$)	
	hFAAH	rFAAH
PF-04457845	40,300 ± 11,500[b]	32,400 ± 8600[b]
PF-3845	12,600 ± 3,000[c]	3900 ± 780[c]
PF-750	791 ± 34[d]	104 ± 14[d]
URB597	1590[c]	-

[a]The k_{inact}/K_i values were obtained in the 384-well format assay as described in "Methods." Values are averages ± SD of at least three independent determinations.

[b](Johnson et al., 2011)

[c](Ahn et al., 2009)

[d](Mileni et al., 2008)

Table 2. **IC_{50} values for FAAH inhibition by PF-04457845 with various preincubation times[a].**

Preincubation time (min)	IC_{50} (nM)	
	hFAAH	rFAAH
1	50.4 ± 5.5	43.1 ± 2.3
15	32.4 ± 0.99	26.7 ± 1.5
30	10.7 ± 1.0	11.1 ± 0.55
60	7.2 ± 0.63	7.4 ± 0.62

[a]The IC_{50} values were obtained in the 384-well format assay as described in "Methods." Values are averages ± SD from three experiments.

Figure 1

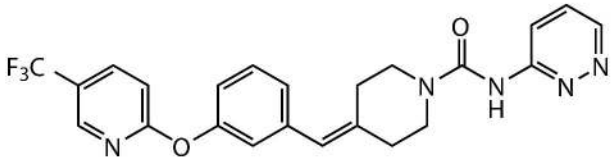

PF-04457845

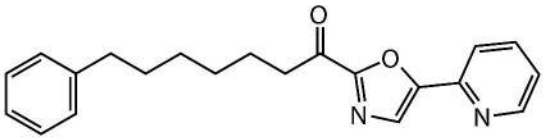

OL-135

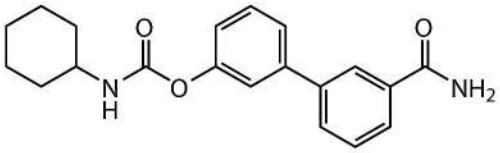

URB597

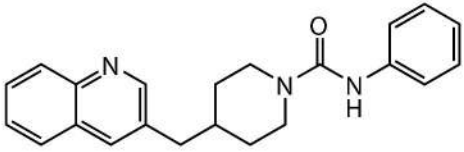

PF-750

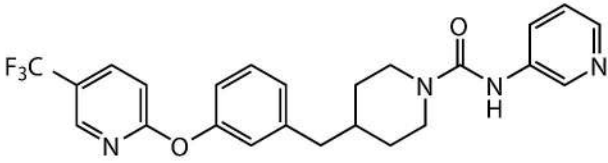

PF-3845

Figure 2

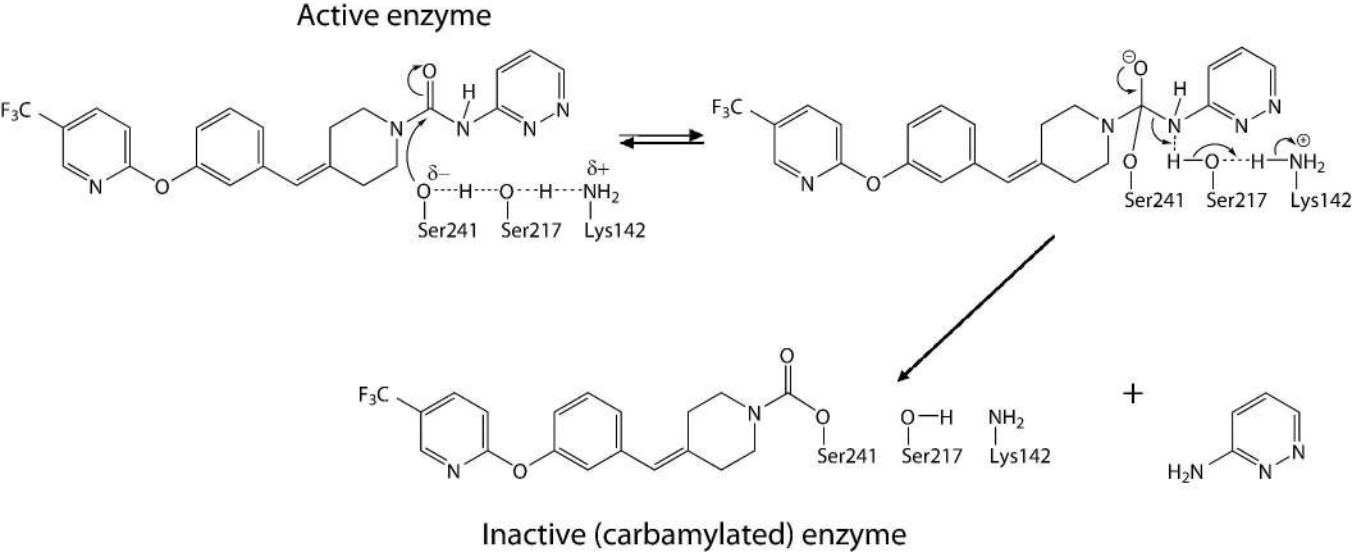
Active enzyme
F3C
N
O
H
N
N
δ–
δ+
O
H
O
H
NH2
Ser241
Ser217
Lys142
Ser241
Ser217
Lys142
Inactive (carbamylated) enzyme
O—H
NH2
H2N

Figure 3

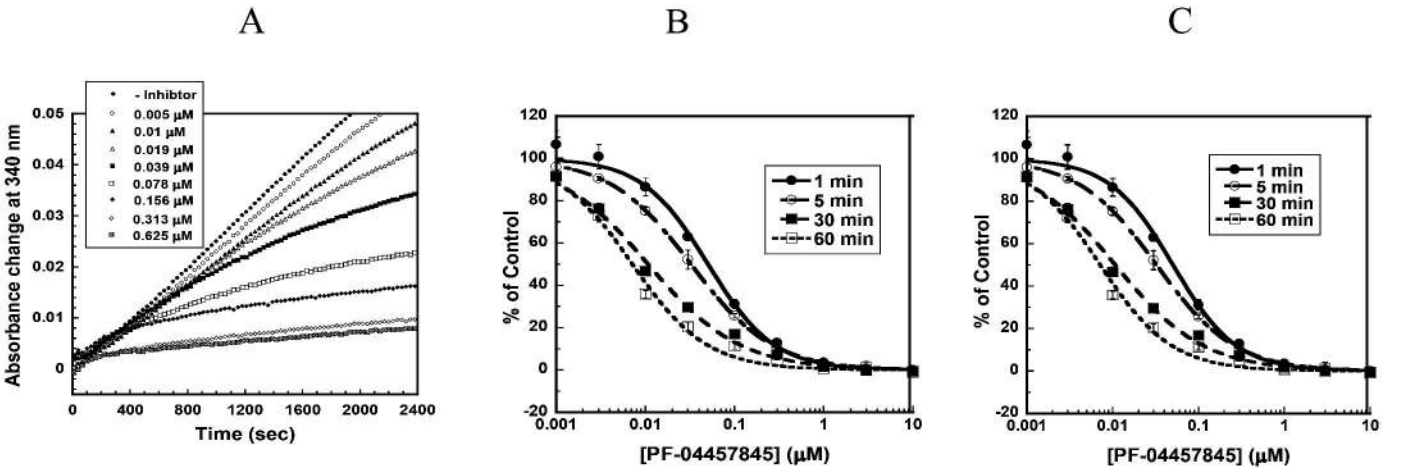
A
B
C
- Inhibtor
0.005 μM
0.01 μM
0.019 μM
0.039 μM
0.078 μM
0.156 μM
0.313 μM
0.625 μM
Absorbance change at 340 nm
Time (sec)
% of Control
[PF-04457845] (μM)
1 min
5 min
30 min
60 min

Figure 4

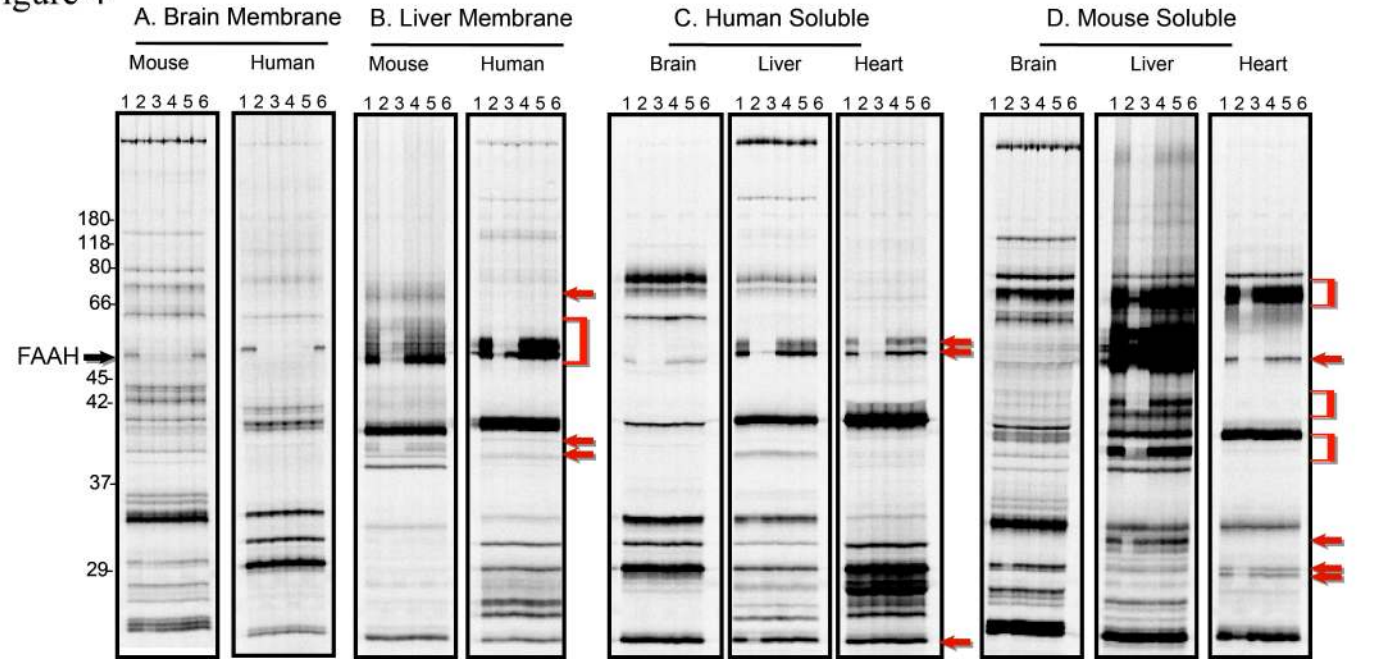
A. Brain Membrane
Mouse
Human
B. Liver Membrane
Mouse
Human
C. Human Soluble
Brain
Liver
Heart
D. Mouse Soluble
Brain
Liver
Heart
1 2 3 4 5 6
180
118
80
66
FAAH
45
42
37
29

Figure 5

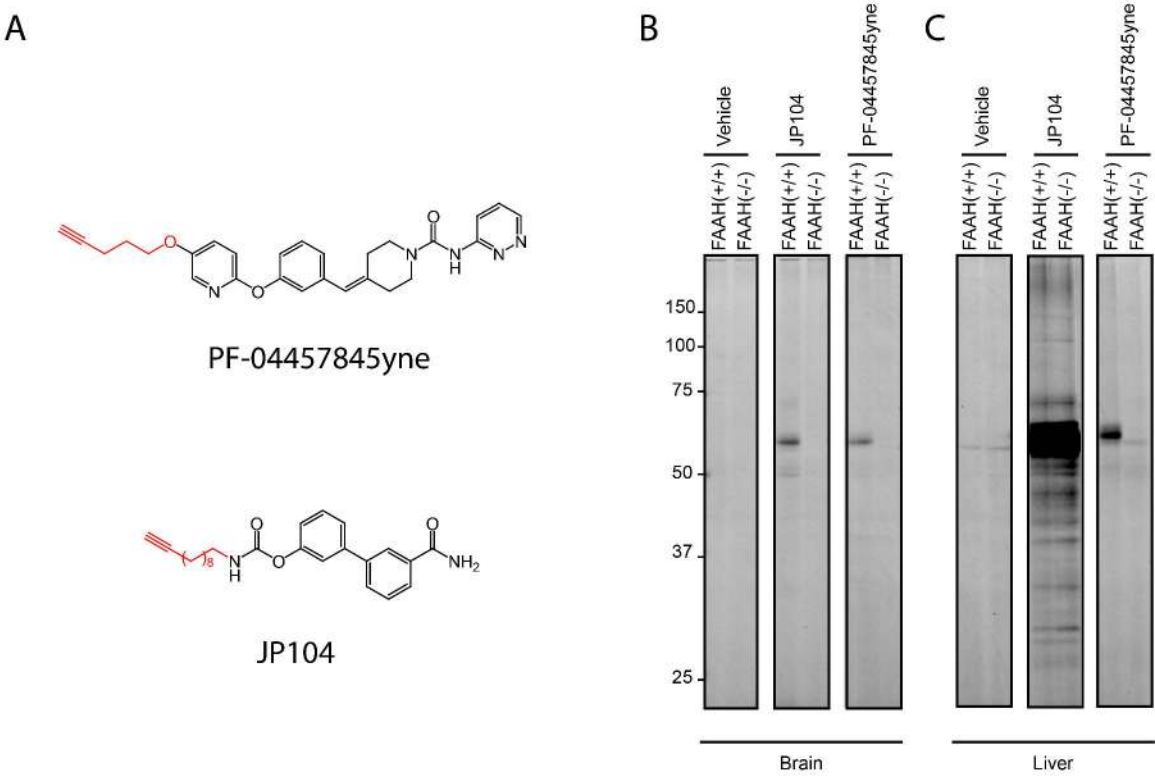
A
PF-04457845yne
JP104
B
C
Vehicle
JP104
PF-04457845yne
FAAH(+/+)
FAAH(-/-)
150
100
75
50
37
25
Brain
Liver

Figure 6

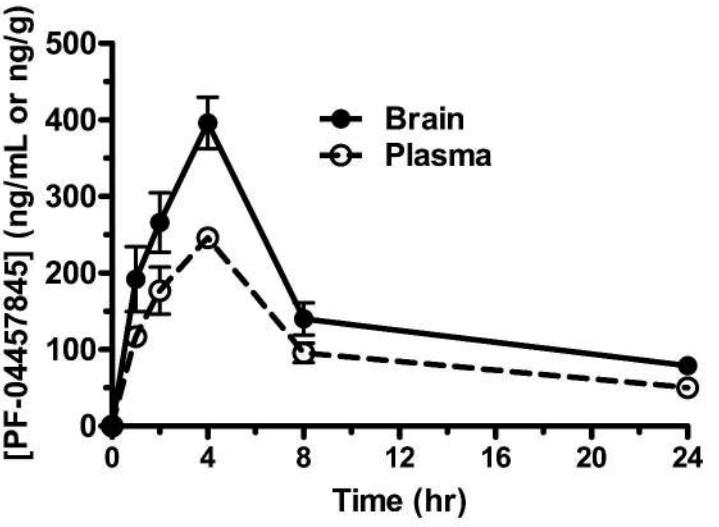
[PF-04457845] (ng/mL or ng/g)
500
400
300
200
100
0
0
4
8
12
16
20
24
Time (hr)
Brain
Plasma

Figure 7

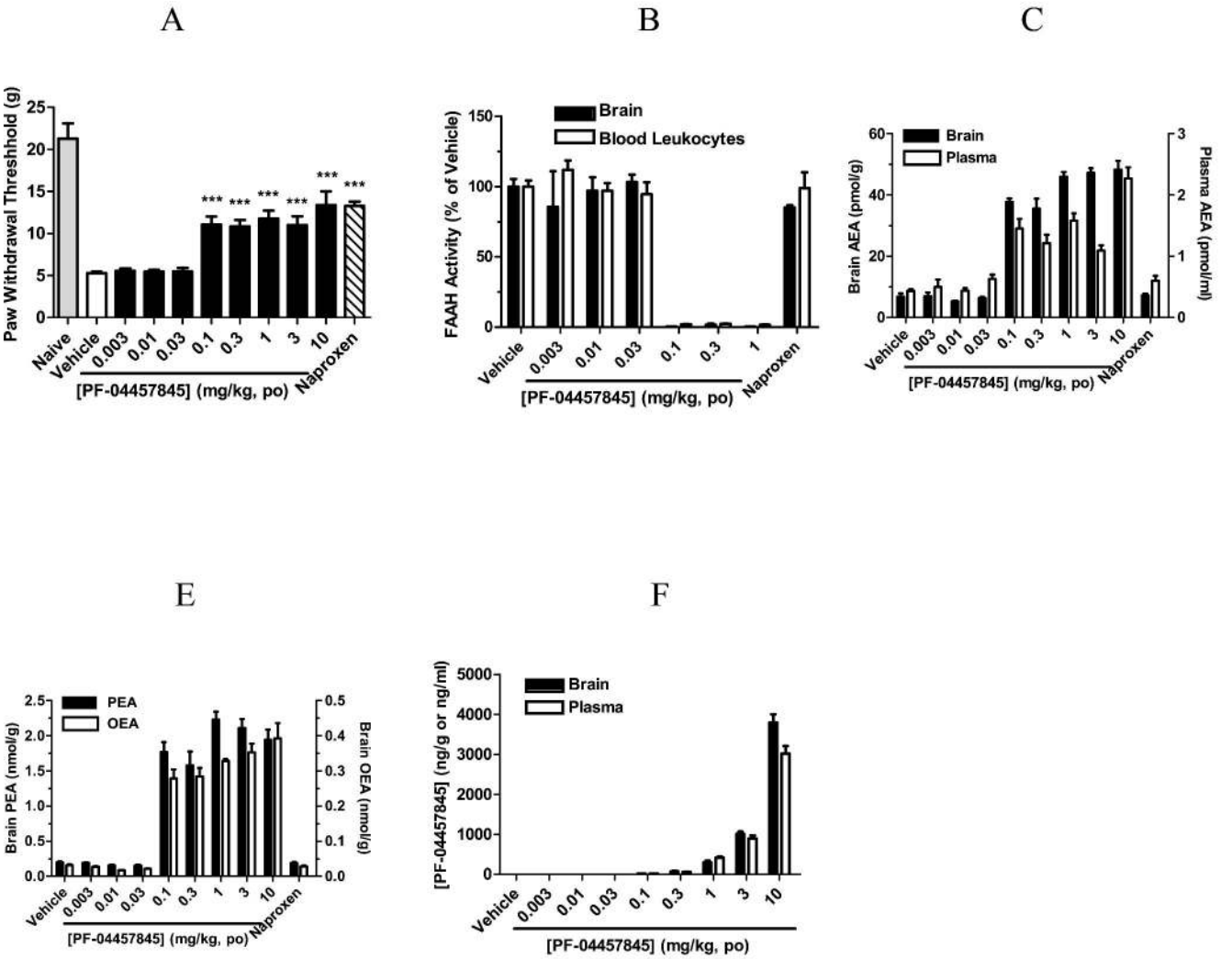
A
B
C
Paw Withdrawal Threshhold (g)
Naive
Vehicle
0.003
0.01
0.03
0.1
0.3
1
3
10
Naproxen
[PF-04457845] (mg/kg, po)
***
FAAH Activity (% of Vehicle)
Brain
Blood Leukocytes
Brain AEA (pmol/g)
Plasma AEA (pmol/ml)
Plasma
E
F
PEA
OEA
Brain PEA (nmol/g)
Brain OEA (nmol/g)
[PF-04457845] (ng/g or ng/ml)

Figure 8

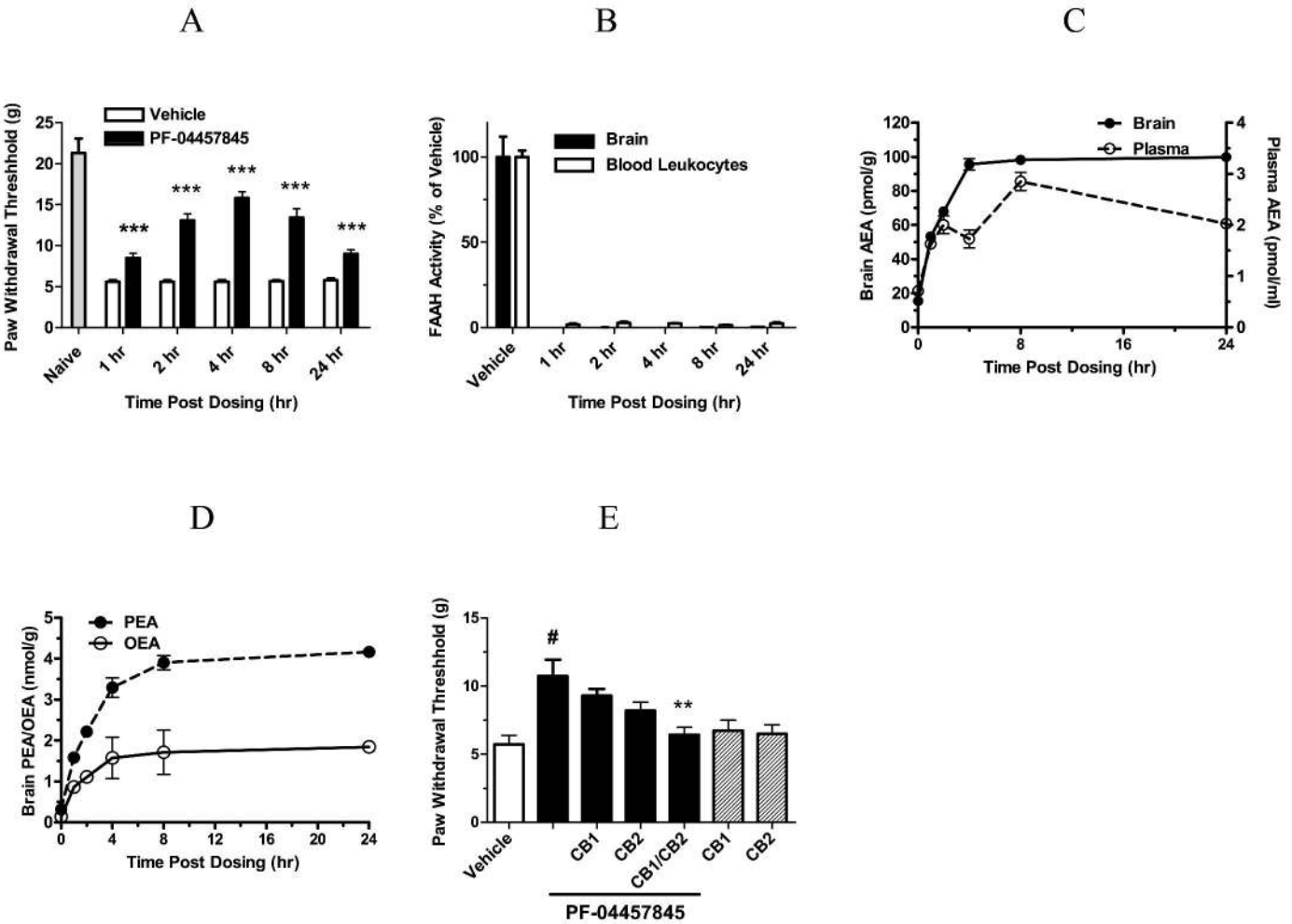
A
Vehicle
PF-04457845
Paw Withdrawal Threshhold (g)
Naive
1 hr
2 hr
4 hr
8 hr
24 hr
Time Post Dosing (hr)
B
Brain
Blood Leukocytes
FAAH Activity (% of Vehicle)
Vehicle
Time Post Dosing (hr)
C
Brain
Plasma
Brain AEA (pmol/g)
Plasma AEA (pmol/ml)
Time Post Dosing (hr)
D
PEA
OEA
Brain PEA/OEA (nmol/g)
Time Post Dosing (hr)
E
Paw Withdrawal Threshhold (g)
Vehicle
CB1
CB2
CB1/CB2
CB1
CB2
PF-04457845

Figure 9

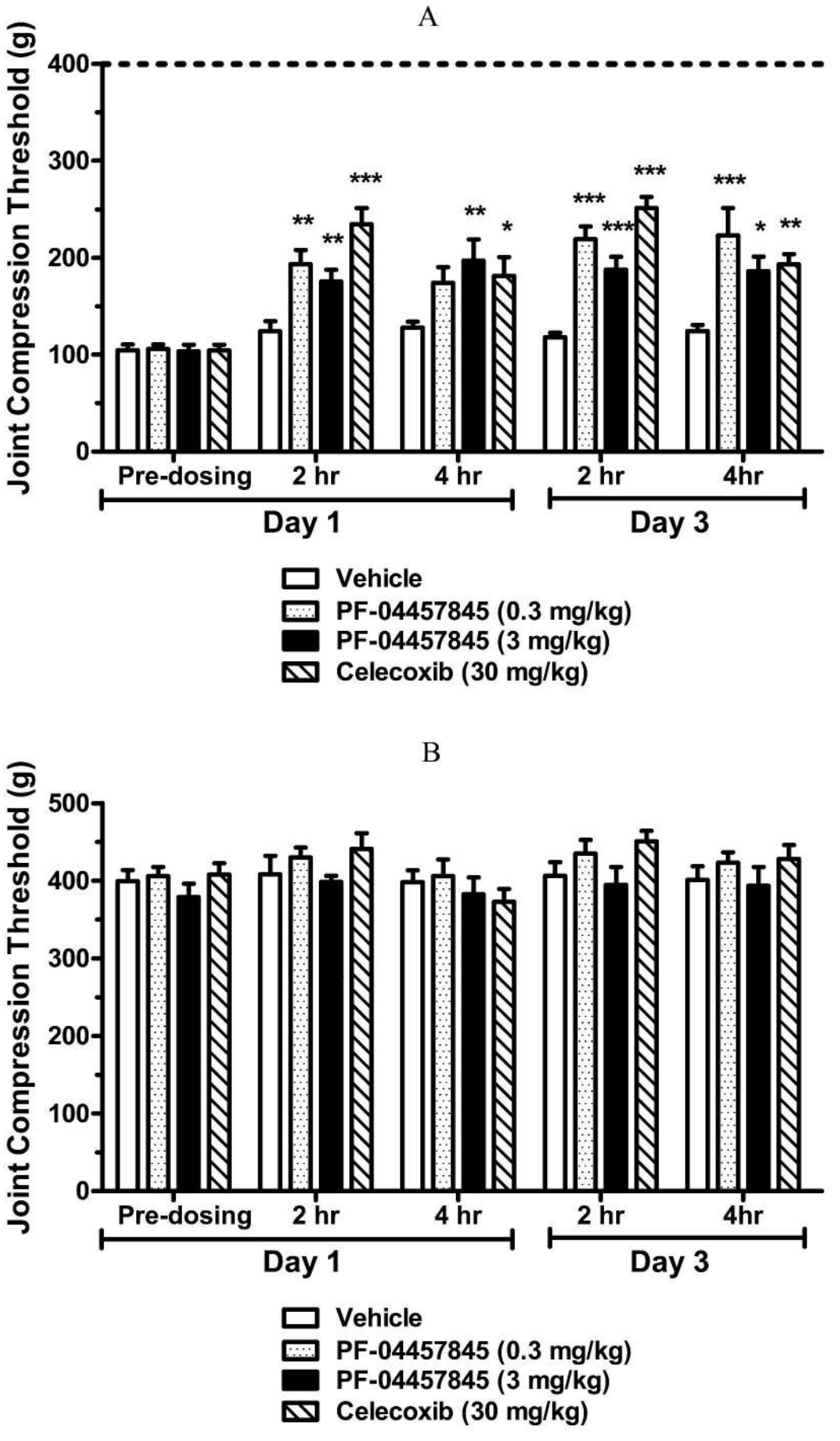
A
Joint Compression Threshold (g)
400
300
200
100
0
**
**
***
**
*
***
***
***
***
*
**
Pre-dosing
2 hr
4 hr
2 hr
4hr
Day 1
Day 3
Vehicle
PF-04457845 (0.3 mg/kg)
PF-04457845 (3 mg/kg)
Celecoxib (30 mg/kg)
B
Joint Compression Threshold (g)
500
400
300
200
100
0
Pre-dosing
2 hr
4 hr
2 hr
4hr
Day 1
Day 3
Vehicle
PF-04457845 (0.3 mg/kg)
PF-04457845 (3 mg/kg)
Celecoxib (30 mg/kg)

Figure 10

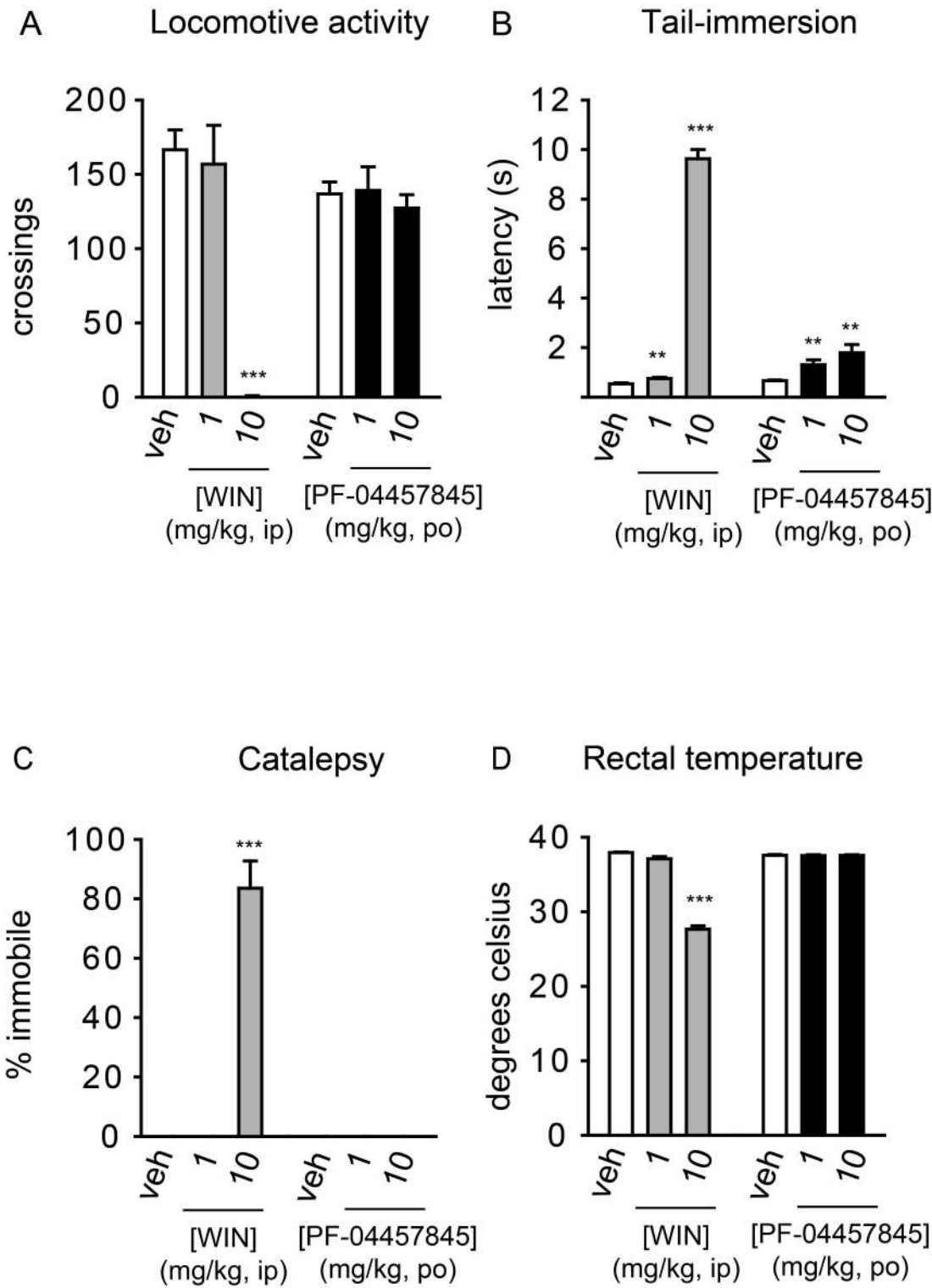
A
Locomotive activity
crossings
200
150
100
50
0
***
veh
1
10
veh
1
10
[WIN]
(mg/kg, ip)
[PF-04457845]
(mg/kg, po)
B
Tail-immersion
latency (s)
12
10
8
6
4
2
***
**
**
**
veh
1
10
veh
1
10
[WIN]
(mg/kg, ip)
[PF-04457845]
(mg/kg, po)
C
Catalepsy
% immobile
100
80
60
40
20
0
***
veh
1
10
veh
1
10
[WIN]
(mg/kg, ip)
[PF-04457845]
(mg/kg, po)
D
Rectal temperature
degrees celsius
40
30
20
10
0
***
veh
1
10
veh
1
10
[WIN]
(mg/kg, ip)
[PF-04457845]
(mg/kg, po)